

TEM-TDEM soundings with the use of vertical loops

V.S. Mogilatov*, A.Yu. No

*A.A. Trofimuk Institute of Petroleum Geology and Geophysics, Siberian Branch of the Russian Academy of Sciences,
3 prosp. Akad. Koptyuga, Novosibirsk, 630090, Russia*

Received 17 December 2008; accepted 29 April 2009

Abstract

In the course of scientific collaboration, we were involved in discussion on the capacity of a vertical loop configuration to resolve thin high-resistivity layers, which is quite an interesting and largely debated point. We report a small forward modeling study including an algorithm based on an analytical solution by separation of variables and a respective program for computing the time-domain TEM field of a horizontal magnetic dipole. We infer that the subsurface vertical loop system shows no critical advantage in resolving thin insulating inclusions.

© 2010, V.S. Sobolev IGM, Siberian Branch of the RAS. Published by Elsevier B.V. All rights reserved.

Keywords: TEM-TDEM method; horizontal magnetic dipole; vertical loop; simulation

Introduction

Currently there exists no simple way in TEM surveys to resolve thin highly resistive layers, though this may be needed, for instance, to explore oil accumulations or to identify salt-bearing formations or asphalts. The problem has no easy and efficient solution in the structural mapping applications, but the required properties may be expected from vertical loop responses in shallow soundings. Theoretically these responses correspond to the horizontal components of the magnetic field excited by a horizontal magnetic dipole (HMD). HMD obviously excites both modes of the electromagnetic field in the earth and, hence, the vertical current. Yet, it remains unclear whether and how far the vertical-loop configuration can resolve thin insulating inclusions.

H and E modes

Below we investigate HMD responses of a layered earth. Let the source (horizontal magnetic dipole) be a specific case of impressed surface magnetic current (Dmitriev, 1968). For each uniform layer ($i = 0, 1, \dots, N$), except the plane ($z = z_0$) with the impressed current, one has to solve the Maxwell equations:

$$\text{rot } \mathbf{H} = \sigma_i \mathbf{E},$$

$$\text{rot } \mathbf{E} = i\omega\mu_0 \mathbf{H},$$

$$\text{div } \mathbf{j} = 0,$$

$$\text{div } \mathbf{H} = 0,$$

where $\mathbf{j} = \sigma_i \mathbf{E}$. The horizontal components of the field (H_x, H_y, E_x, E_y) are continuous at the layer boundaries. The conditions at the boundary $z = z_0$ which contains the surface impressed current (with the surface current density, A), are

$$[E_x] \Big|_{z=z_0} = i\omega\mu_0 \cdot j_y^M(x, y),$$

$$[E_y] \Big|_{z=z_0} = -i\omega\mu_0 \cdot j_x^M(x, y),$$

(1)

$$[H_x] \Big|_{z=z_0} = 0,$$

$$[H_y] \Big|_{z=z_0} = 0.$$

Hereafter $[F] \Big|_{z=z_i}$ denotes the jump of the F function on passage through $z = z_i$, i.e., the source is included as an additional boundary condition in the general problem for the total field.

The total field is divided into magnetic and electric modes, and the horizontal components are expressed via the vertical components as

* Corresponding author.

E-mail address: MogilatovVS@ipgg.nsc.ru (V.S. Mogilatov)

$$\begin{aligned} \frac{\partial H_y}{\partial x} - \frac{\partial H_x}{\partial y} &= \sigma_i E_z, \\ \frac{\partial E_y}{\partial x} - \frac{\partial E_x}{\partial y} &= i\omega\mu_0 H_z, \\ \frac{\partial H_x}{\partial x} + \frac{\partial H_y}{\partial y} &= -\frac{\partial H_z}{\partial z}, \\ \frac{\partial E_x}{\partial x} + \frac{\partial E_y}{\partial y} &= -\frac{\partial E_z}{\partial z}, \end{aligned} \tag{2}$$

E_z and H_z in each layer ($z \neq z_0$) should satisfy the equations

$$\frac{\partial^2 E_z}{\partial x^2} + \frac{\partial^2 E_z}{\partial y^2} + \frac{\partial^2 E_z}{\partial z^2} - k_i^2 \cdot E_z = 0, \tag{3}$$

$$\Delta H_z - k_i^2 H_z = 0,$$

where $k_i^2 = -i\omega\mu_0\sigma_i$. Taking into account (1) and (2), at layer boundaries ($z = z_i, i = 1, 2, \dots, N$) and at the boundary with the source ($z = z_0$) we have

$$[\sigma E_z] \Big|_{z=z_0, z_i} = \left[\frac{\partial H_y}{\partial x} - \frac{\partial H_x}{\partial y} \right] \Big|_{z=z_0, z_i} = 0, \tag{4}$$

$$\left[\frac{\partial E_z}{\partial z} \right] \Big|_{z=z_0, z_i} = \begin{cases} -i\omega\mu_0 \text{rot}_z \mathbf{j}^M, & z = z_0, \\ 0, & z = z_i, \end{cases} \tag{5}$$

$$[H_z] \Big|_{z=z_0, z_i} = \begin{cases} -\text{div} \mathbf{j}^M, & z = z_0, \\ 0, & z = z_i, \end{cases} \tag{6}$$

$$\left[\frac{\partial H_z}{\partial z} \right] \Big|_{z=z_0, z_i} = - \left[\frac{\partial H_x}{\partial x} + \frac{\partial H_y}{\partial y} \right] \Big|_{z=z_0, z_i} = 0. \tag{7}$$

In addition to the conditions of (3)–(7), there are the radiation conditions for the functions E_z, H_z . Thus, we have two independent problems, which share the common source \mathbf{j}^M but have different dependences. The two problems are solved by separation of variables. Inasmuch as the problem in general has no symmetry (the distribution $\mathbf{j}^M(x, y)$ remains arbitrary), the variables are separated using the 2D Fourier transform along x and y :

$$f(x, y, z) = \frac{1}{(2\pi)^2} \iint_{-\infty}^{\infty} f^*(\xi, \eta, z) e^{i(\xi x + \eta y)} d\xi d\eta,$$

$$f^*(\xi, \eta, z) = \iint_{-\infty}^{\infty} f(x, y, z) e^{-i(\xi x + \eta y)} dx dy.$$

In the axisymmetrical case, when the function f depends uniquely on $r = \sqrt{x^2 + y^2}$ a pair of double Fourier transforms is equivalent to a pair of Hankel transforms:

$$f(r, z) = \frac{1}{2\pi} \int_0^{\infty} f^*(\lambda, z) J_0(\lambda r) \lambda d\lambda,$$

$$f^*(\lambda, z) = 2\pi \int_0^{\infty} f(r, z) J_0(\lambda r) r dr.$$

where $\lambda = \sqrt{\xi^2 + \eta^2}$.

Now we proceed to the Fourier image of the problem. In the transformation of boundary conditions (5), (6), which allow for the presence of the source in the plane $z = z_0$, one has to determine the integrals

$$D^* = \iint_{-\infty}^{\infty} \text{div} \mathbf{j}^M(x, y) e^{-i\xi x} e^{-i\eta y} dx dy, \tag{8}$$

$$R^* = \iint_{-\infty}^{\infty} \text{rot}_z \mathbf{j}^M(x, y) e^{-i\xi x} e^{-i\eta y} dx dy.$$

Then, taking into account the conditions for H_z and E_z (3)–(7) and (8), the H_z and E_z images in each layer are found as

$$E_z^*(z, \xi, \eta) = -\frac{i\omega\mu_0}{2\lambda} V(z, \lambda) R^*(\xi, \eta), \tag{9}$$

$$H_z^*(z, \xi, \eta) = -\frac{1}{2} X(z, \lambda) D^*(\xi, \eta).$$

The problems for H_z and E_z (3)–(7) are transformed in a necessary and sufficient way into the following boundary-value problems for two functions X and V that are quite independent of each other and of the source configuration (in plan)

for function X :

$$X''_{zz} - u_i^2 X = 0,$$

$$[X] \Big|_{z=z_0, z_i} = \begin{cases} 2, & z = z_0, \\ 0, & z = z_i, \end{cases}$$

$$[X'_z] \Big|_{z=z_0, z_i} = 0,$$

$$X \rightarrow 0,$$

for function V :

$$V''_{zz} - u_i^2 V = 0, \quad -\infty < z < \infty,$$

$$[\sigma V] \Big|_{z=z_0, z_i} = 0, \tag{10}$$

$$[V'_z] = \begin{cases} 2\lambda, & z = z_0, \\ 0, & z = z_i, \end{cases}$$

$$V \rightarrow 0, \quad |z| \rightarrow \infty,$$

where $u_i^2 = \lambda^2 + k_i^2, z_i (i = 1, 2, \dots, N)$ are the coordinates of the boundaries of uniform layers and z_0 is the source position.

As for the horizontal components, applying the Fourier transform for (2) and substituting the equations for E_z^* and H_z^* (9) gives

$$H_x^* = \bar{\eta} \frac{k_i^2}{2\lambda} V R^* - \bar{\xi} \frac{1}{2} X'_z D^*,$$

$$H_y^* = -\bar{\xi} \frac{k_i^2}{2\lambda} VR^* - \bar{\eta} \frac{1}{2} X_z' D^*,$$

$$E_x^* = -\frac{i\omega\mu_0}{2} \left[\bar{\xi} \frac{1}{\lambda\Lambda_i^2} V_z' R^* - \bar{\eta} X D^* \right],$$

$$E_y^* = -\frac{i\omega\mu_0}{2} \left[\bar{\eta} \frac{1}{\lambda} V_z' R^* - \bar{\xi} X D^* \right],$$

where $\bar{\xi} = i\xi/\lambda^2$, $\bar{\eta} = i\eta/\lambda^2$.

Solving boundary-value problems

When solving boundary-value problems (10), the functions X and V in each uniform layer (assuming $(z = z_0)$ to be the boundary) are expressed as follows, according to the equations and conditions (10) (the Z axis is directed downward)

$$F(z) = A_0 \cdot \exp(u_0 z), \quad z < 0,$$

$$F(z) = A_i \cdot \exp(u_i z) + B_i \cdot \exp(-u_i z), \quad z_i < z < z_{i+1},$$

$$F(z) = B_N \cdot \exp[-u_N(z - z_N)], \quad z > z_N.$$

In (12) F denotes any function X or V . It is convenient to present the solution inside a layer of a finite thickness $(z_i < z < z_{i+1})$ in a different form using the values of the function and its derivative at the boundary (from inside). Defining A_i and B_i in the equations as

$$F(z_i) = A_i \cdot \exp(u_i z) + B_i \cdot \exp(-u_i z),$$

$$F'_x(z_i) = A_i u_i \cdot \exp(u_i z) - B_i u_i \cdot \exp(-u_i z),$$

gives

$$F(z) = F_i \cdot \cosh[u_i(z - z_i)] + \frac{F'_i}{u_i} \sinh[u_i(z - z_i)],$$

$$F'_z(z) = F_i u_i \cdot \sinh[u_i(z - z_i)] + F'_i \cosh[u_i(z - z_i)],$$

which allows extrapolating the function and its derivative at the i th boundary downward into the values at any z in the given layer, specifically, at $z = z_{i+1}$, i.e., at the next boundary. In the same way, one can also express the solution via F_{i+1} , F'_{i+1} at the lowermost boundary and obtain a possibility to “move up”. Thus, it is possible to achieve the solution in each layer moving downward as far as the source to an accuracy of the coefficient A_0 . Or, in the same way, one can find the solution in each layer moving upward as far as the source to the B_N accuracy. The coefficients A_0 and B_N can be found by reconciling the two solutions at the source-bearing boundary.

Introducing the functions $\zeta(z)$ which are independent of the source position, we obtain $F(z) = A_0 \cdot \overset{\vee}{\zeta}(z)$ above the boundary with the impressed magnetic current $(z < z_0)$ in the downward direction

$$\overset{\vee}{\zeta}(z) = \exp(u_0 z), \quad z < 0,$$

for $z_i < z < z_{i+1}$:

$$\overset{\vee}{\zeta}(z) = \overset{\vee}{\zeta}_i \cosh[u_i(z - z_i)] + \frac{\overset{\vee}{\zeta}'_i}{u_i} \sinh[u_i(z - z_i)],$$

$$\overset{\vee}{\zeta}(z) = \overset{\vee}{\zeta}_i u_i \sinh[u_i(z - z_i)] + \overset{\vee}{\zeta}'_i \cosh[u_i(z - z_i)],$$

where $\overset{\vee}{\zeta}_i = \overset{\vee}{\zeta}(z_i)$, $\overset{\vee}{\zeta}'_i = \overset{\vee}{\zeta}'_z(z_i)$.

The function $F(z) = B_N \cdot \overset{\wedge}{\zeta}(z)$ below the source $(z > z_0)$ is calculated in the same way, but $\overset{\wedge}{\zeta}(z)$ is found in the upward direction

$$\overset{\wedge}{\zeta}(z) = \exp[-u_N(z - z_N)], \quad z > z_N,$$

for $z_i < z < z_{i+1}$:

$$\overset{\wedge}{\zeta}(z) = \overset{\wedge}{\zeta}_{i+1} \cosh[u_i(z - z_{i+1})] + \frac{\overset{\wedge}{\zeta}'_{i+1}}{u_i} \sinh[u_i(z - z_{i+1})],$$

$$\overset{\wedge}{\zeta}(z) = \overset{\wedge}{\zeta}_{i+1} u_i \sinh[u_i(z - z_{i+1})] + \overset{\wedge}{\zeta}'_{i+1} \cosh[u_i(z - z_{i+1})],$$

where $\overset{\wedge}{\zeta}_i = \overset{\wedge}{\zeta}(z_i)$, $\overset{\wedge}{\zeta}'_i = \overset{\wedge}{\zeta}'_z(z_i)$.

On transition through simple boundaries the following functions are continuous

for X : for V :

$$h = \zeta \text{ and } f = \zeta'_z/\lambda, \quad f = \sigma\zeta \text{ and } h = \zeta'_z/\lambda.$$

The function F is found, with the source at $z = z_0$, from the coefficients A_0 and B_N , taking into account the conditions at this boundary, according to (10):

$$F(z) = \frac{2\hat{f}(z_0) \overset{\vee}{\zeta}(z)}{D}, \quad z < z_0 \text{ (above source),}$$

$$F(z) = \frac{2\overset{\vee}{f}(z_0) \overset{\wedge}{\zeta}(z)}{D}, \quad z > z_0 \text{ (below source),}$$

and

$$F'_z(z) = \frac{2\hat{f}(z_0) \overset{\vee}{\zeta}'_z(z)}{D}, \quad z < z_0 \text{ (above source),}$$

$$F'_z(z) = \frac{2\overset{\vee}{f}(z_0) \overset{\wedge}{\zeta}'_z(z)}{D}, \quad z > z_0 \text{ (below source),}$$

where $(\overset{\vee}{\cdot})$ means that the function is defined from above the source, successively downward, by (14); $(\overset{\wedge}{\cdot})$, correspondingly, means that the function is defined from below the source, successively upward from the bottom of the lowermost boundary, by (15):

$$D = \overset{\vee}{f}(z_0) \hat{h}(z_0) - \hat{f}(z_0) \overset{\vee}{h}(z_0).$$

Horizontal magnetic dipole

Now we consider a horizontal magnetic dipole placed at z_0 on the Z axis, with its moment along the X axis. In this case, the 2D current distribution, which we have assumed so far to be arbitrary, becomes

$$j_x^M = M_x \cdot \delta(x) \cdot \delta(y), \quad j_y^M = 0,$$

where M_x is the moment. Then,

$$\text{rot}_z \mathbf{j}^M = -M_x \cdot \delta(x) \cdot \delta'(y), \quad \text{div} \mathbf{j}^M = M_x \cdot \delta'(x) \cdot \delta(y).$$

Therefore, we obtain the following specific equations for the functions R^* and D^* , according to (8), using the properties of the Dirac delta function:

$$R^* = -M_x \cdot (\mathbf{i}\eta), \quad D^* = M_x \cdot (\mathbf{i}\xi).$$

The images of the sought HMD field components, i.e., H_z^* and H_x^* , become

$$H_z^* = -\frac{M_x}{2} X \cdot (\mathbf{i}\xi),$$

$$H_x^* = -\frac{M_x}{2} \cdot \left[\left(\frac{\mathbf{i}\eta}{\lambda} \right)^2 \cdot \frac{k^2}{\lambda} \cdot V + \left(\frac{\mathbf{i}\xi}{\lambda} \right)^2 \cdot X'_z \right].$$

For the originals, applying the Fourier transform gives

$$H_z = -\frac{M_x}{4\pi} \cdot \frac{\partial}{\partial x} \int_0^\infty J_0(\lambda r) \lambda X d\lambda,$$

$$H_x = -\frac{M_x}{4\pi} \cdot \left[k^2 \frac{\partial^2}{\partial y^2} \int_0^\infty J_0(r\lambda) \frac{V}{\lambda^2} d\lambda + \frac{\partial^2}{\partial x^2} \int_0^\infty J_0(r\lambda) \frac{X'_z}{\lambda} d\lambda \right].$$

Finally, in the case of the solution on the X axis ($y = 0, x \equiv r$)

$$H_z = \frac{M_x}{4\pi} \int_0^\infty J_1(\lambda r) \lambda^2 X d\lambda,$$

$$H_x = -\frac{M_x}{4\pi r} \cdot \left\{ k^2 \int_0^\infty J_1(\lambda r) \frac{V}{\lambda} d\lambda + \int_0^\infty [J_0(\lambda r)\lambda r + J_1(\lambda r)] X'_z d\lambda \right\}. \tag{18}$$

Now we consider the equation for H_x , where $k^2 = -i\omega\mu_0\sigma$ has been determined for the observation point, but the system—and, hence, the observation point—are in the non-conducting air, where $\sigma = 0$ and, hence, $k^2 = 0$. Then,

$$H_x = \frac{M_x}{4\pi r} \cdot \left\{ \int_0^\infty [J_0(\lambda r)\lambda r + J_1(\lambda r)] X'_z d\lambda \right\}.$$

However, this means that the field is induced uniquely by horizontal secondary currents while the vertical current does not contribute to the air magnetic field. This casts doubt whether vertical-loop surveys can resolve thin resistive layers in the subsurface. For better understanding, we are to analyze the case numerically.

Horizontal magnetic dipole on the surface of a uniform earth

The solution in the case of a uniform earth model can be represented as simple functions. These simple equations will be useful in designing and testing the general algorithm.

The equation for the HMD response is selected from the above general formulas for a layered earth. Using the general algorithm, for the horizontal magnetic dipole on the surface of a uniform earth with the resistivity ρ , we obtain

$$H_x = -\frac{M_x}{2\pi} \frac{\partial^2}{\partial x^2} \int_0^\infty J_0(\lambda x) \frac{\rho}{\lambda + p} d\lambda, \tag{19}$$

where $p^2 = \lambda^2 + k^2, k^2 = -i\omega\mu/\rho, \mu$ being the magnetic permeability.

This integral known from (Van'yan, 1965) leads to

$$H_x(\omega) = \frac{M_x}{2\pi} \left[-\frac{2}{x^3} + \frac{12}{k^2 x^5} - \frac{e^{-kx}}{k^2 x^5} (12 + 12kx + 5k^2 x^2 + k^3 x^3) \right]. \tag{20}$$

The time-domain response is found using the Fourier transform. For the practical purpose, one needs the time derivative \dot{B}_x where $B_x = \mu H_x$. Thus, one has to calculate the integral

$$\dot{B}_x(t) = \frac{\mu}{2\pi} \int_{-\infty}^\infty e^{-i\omega t} H_x(\omega) d\omega,$$

where H_x is according to (18). Integrals of this kind have been explored in detail in (Van'yan, 1965), and we obtain

$$\dot{B}_x = \frac{M_x \rho}{2\pi x^5} \left\{ 12 \cdot \Phi(u) - \sqrt{\frac{2}{\pi}} e^{-u^2/2} (12u + 4u^3 + u^5) \right\} \tag{21}$$

where $u = r\sqrt{\frac{\mu}{2\rho t}}, \Phi(z) = \sqrt{\frac{2}{\pi}} \int_0^z e^{-x^2/2} dx.$

Program for computing HMD transient responses of an N -layer earth

In the general case, integration (18) cannot be analytical but requires numerical calculation. For this we have designed the MAGXX program (FORTRAN) using the above algorithm. While making the program, we struck on a difficulty which is common in problems of this kind: there is not enough

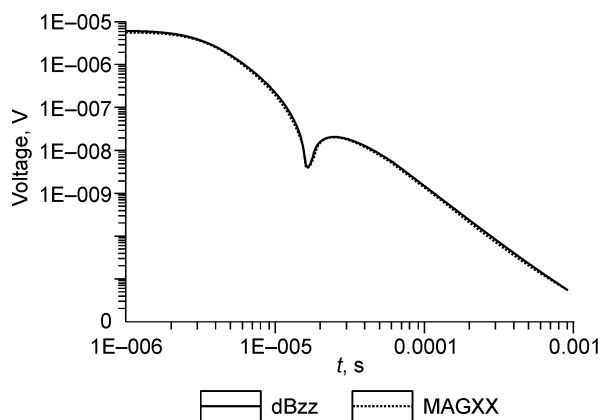


Fig. 1. Suggested program (dBzz) and testing program (MAGXX), compared.

decay at $\lambda \rightarrow \infty$ in integrals (18), when the transmitter and the receiver are placed on the same boundary. The convergence was improved with the known procedure of subtracting the integrand function for halfspace (19) and adding the respective function in time domain (21) after all integrations. Numerical integration was performed by the Gauss method (Il'in, 2004).

The program was tested nontrivially, but only in the time domain for the lack of opportunity of doing it in the frequency domain. The testing program was one for TEM logging designed at the Laboratory of Electromagnetic Fields of the A.A. Trofimuk Institute of Petroleum Geology and Geophysics (Novosibirsk) for computing the voltage generated by a system inserted into a conducting subsurface. The upper halfspace (air) was simulated by a high finite resistance, and the system was shifted 1 cm down. With this shift, the TEM field change only slightly at a loop spacing of several meters. These conditions created strong algorithmic stress for the testing program itself. Nevertheless, our program and the testing program showed quite a satisfactory fit (Fig. 1).

The fact that the frequency-domain procedure is amenable to the standard numerical Fourier transformation into the time

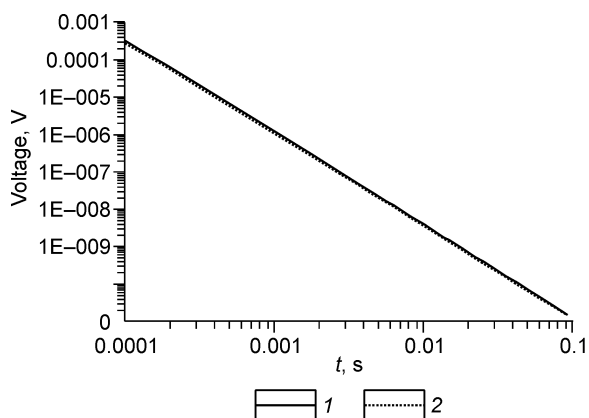


Fig. 3. Responses of a three-layer earth with a thin resistive second layer and of a uniform earth. 1, uniform earth, 2, thin layer, $h = 1$ m.

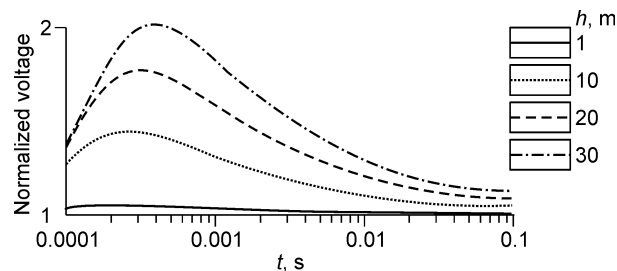


Fig. 2. Responses of a layered earth with constant transverse resistivity of second layer, normalized to uniform-earth responses.

domain, which is broadly used in data processing software for resistivity surveys, such as Podbor or Vybor-ZS (Mogilatov, 2002), allows us to treat the results as reliable.

Numerical experiments

Now we possess a program to check numerically the efficiency of the vertical loop configuration in exploring thin resistive layers in the subsurface. The respective numerical experiments and the results are reported below.

The selected model consists of a three-layer section with the second layer of a constant transverse resistivity ($\rho h = \text{const}$). The model parameters were initially $\rho = 100$ Ohm m, $h = 30$ m, and then the layer thickness was lowered successively ($h = 25, 20, 15, 10, 5, 1$ m) and the resistivity increased to reach the product $\rho_i \cdot h_i = 3000$ Ohm m m. The transient responses of the earth of this kind, compared with the response of a uniform earth, were as follows (Fig. 2).

In each experiment, the curves were normalized to the uniform-earth response. As the layer thinned down, its influence was decreasing though the resistivity increased. The effect from a 1 m thick resistive layer was almost zero, such that the ratio approached the unity and the field almost coincided with that of the uniform halfspace (Fig. 3).

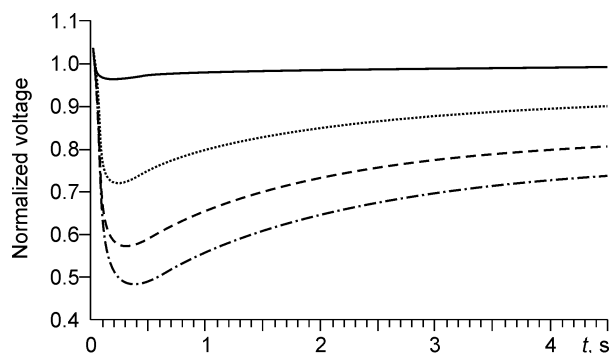


Fig. 4. Horizontal loop responses of a layered earth with constant transverse resistivity of second layer, normalized to uniform-earth responses. Symbols same as in Fig. 2.

Similar experiments were undertaken for a horizontal loop configuration, using the *Podbor* program (Mogilatov, 2002). As we expected, the influence of the resistive layer became progressively lower as its thickness decreased, the resistivity being invariable (Fig. 4).

Thus, the signals from thin resistive layers are very low in both horizontal and vertical loop data. The vertical loop configuration is as inefficient as the horizontal-loop one in resolving high-resistivity subsurface layers.

Conclusions

According to the reported results, the system with a vertical loop on the ground surface (and above it) has no advantage over the classical horizontal-loop configuration in resolving thin resistive layers. The theory predicts that this configuration is inefficient being placed in a nonconducting medium (air). Vertical currents responding to thin resistive objects do arise

but they pay no contribution to the response recorded in the air. A vertical-loop system placed in a medium with finite resistivity is able to resolve thinly layered subsurface sections. For instance, a vertical loop immersed in water may be useful in shelf petroleum exploration, but this application requires further investigation.

References

- Dmitriev, V.I., 1968. A general method for calculating the electromagnetic field in a layered medium, in: *Vychislitelnye Metody i Programirovanie* [in Russian]. MGU, Moscow, Issue 10, pp. 55–65.
- Il'in, V.P., 2004. *Numerical Analysis* [in Russian]. IVMiMG SO RAN, Novosibirsk, Book 1.
- Mogilatov, V.S., 2002. *Frequency Induction Resistivity Surveys* [in Russian]. NGU, Novosibirsk.
- Van'yan, L.L., 1965. *Fundamentals of Electromagnetic Soundings* [in Russian]. Nedra, Moscow.

Editorial responsibility: M.I. Epov